Poisson multi-Bernoulli mixture filtering with an active sonar using BELLHOP simulation

Alexey Narykov*, Michael Wright*, Ángel F. García-Fernández*†, Simon Maskell*, and Jason F. Ralph*
*Dept. of Electrical Engineering and Electronics, University of Liverpool, UK
†ARIES Research Center, Universidad Antonio de Nebrija, Madrid, Spain
Emails: {a.narykov, m.j.wright, angel.garcia-fernandez, smaskell, jfralph}@liverpool.ac.uk

***Abstract*—This paper examines the use of Poisson multi-Bernoulli mixture (PMBM) filters with realistic signal propagation models for tracking of targets with active sonar systems. In particular, the paper considers application of BELLHOP simulation to model the spatial dependence of the target probability of detection. The intention is to develop practical approaches to the problem of accurately representing sonar propagation within an advanced tracking filter.**

***Index Terms*—Poisson multi-Bernoulli mixture filter, sonar tracking, BELLHOP modelling.**

I. Introduction

Mutli-target tracking is the problem of recursively estimating the state of a multi-target system from a stream of noisy measurements in presence of detection failures and false alarms. For a long time, the Multi-Hypothesis Tracker (MHT) [1] has been the industrial standard for multi-target tracking. More recently, new optimal solutions have been developed, with the Poisson multi-Bernoulli Mixture (PMBM) filter [2], [3] offering a Bayesian interpretation of the MHT algorithm, and the relevant connections between algorithms established in [4]. Such algorithms hold a promise of handling data from any sensor should the model of its performance be available to the filter.

This paper is dedicated to target tracking for measurements collected by an active sonar. Such a sensor interrogates its environment by transmitting acoustic waves and extracts information on the targets populating the environment from reflections received by an array of hydrophones (receivers) [5]. From a tracking perspective, modelling of sonar performance amounts to constructing a probabilistic model that describes how the sonar receivers generate target measurements, along with characterising detection failures and possible false alarms.

In particular, we shall be focused on modelling sonar detection performance which varies significantly across the surveillance area. The probability of target detection will be determined by the strength of the reflected signal received at the hydrophone array. Commonly signal-to-noise ratio (SNR) in sonar is modelled for straight line wave propagation, thus making it possible to express it analytically as a simple function of range [6], [7], [8]. In general, however, sonar waves do not propagate in straight lines [9], which turns the probability of detection into a function of the path taken by the propagating wave or waves. Multiple propagation paths are very common in underwater acoustics and this gives rise to significant echoes and interference at the receivers; a problem that is exacerbated for active sonar because propagation paths to and from the target need to be included in the analysis. This makes it difficult to characterise active sonar measurements and leads to problems when characterising these measurements for modern Bayesian tracking methods.

In this work we are interested in the effect of a sonar detection model on the performance of a multi-target tracking algorithm. The approach taken in this paper is to simulate wave propagation and the strength of received signal using the widely used BELLHOP ray tracing model [10], and making its output available to the multi-target filtering algorithm. We consider sonar surveillance with a receiver array in shallow water that provides target range and azimuth information, see e.g., [11], [12].

In a tracking algorithm, the probability of target detection may need to be evaluated for a significant number of possible target locations. For a BELLHOP model, this could render the tracking function prohibitively expensive in terms of computational costs. To alleviate this issue, we employ a particular implementation of the PMBM filter [13] that requires a small and fixed number of characteristic locations (per target update) at which the probability of detection needs to be evaluated.

The contribution of this paper is the integration of the BELLHOP ray tracing model for sonar detection performance with a PMBM filter. It compares the resulting tracking performance to that obtained using uniform probability of detection in the filter, as commonly assumed in multi-target tracking with sonar, see e.g., [7], [14], [15].

The paper is organised as follows. In Section II, a Gaussian implementation of the PMBM filter is reviewed. Section III describes a probabilistic model of sonar surveillance, including the dependency of detection performance on the signal-to-noise conditions. Section IV explains the basics of BELLHOP and its application to modelling the propagation of active sonar signals via ray tracing. Section V presents the experimental results and performance assessment of the developed approach. Section VI concludes the paper.

II. Background

This section presents the background material. We aim to integrate a model of sonar detection performance within the framework of Section II-A to represent state-dependent probability of detection $p_D(\cdot)$. Section II-B reviews the PMBM filter.

A. Filtering assumptions

We consider a probabilistic model using the standard multi-target assumptions [16]. Given the set X_k of targets at time step k, each target $x \in X_k$ survives with a probability $p^S(x)$ and its kinematic state evolves according to transition density $g(\cdot|x)$, or dies with probability $1 - p^S(x)$. This formalism is equally appropriate for describing moving as well as stationary targets. New targets are born according to a Poisson point process (PPP) with intensity $\lambda^B(\cdot)$.

At time step k, each $x \in X_k$ is detected with a probability $p^D(x)$ and generates a measurement with density $l(\cdot|x)$, or is misdetected with probability $1 - p^D(x)$. In other words, it is assumed that each target produces at most a single measurement, and that no measurement is generated by more than a single target, i.e., there are no unresolved targets. Furthermore, detectability of a target is unaffected by the presence of other targets, e.g., there are no occlusions induced by other targets. That is, the model assumes that targets are small compared to the sensor resolution. False alarms are modelled as a PPP with intensity $\lambda^{\text{FA}}(\cdot)$.

B. Poisson Multi-Bernoulli Mixture Filter

The posterior of X_k is calculated via the PMBM filter [3], [17]. This filter maintains information on the multi-target situation in a form of the Poisson multi-Bernoulli Mixture (PMBM) density $f_{k'|k}(\cdot)$. This density describes the set of targets at time step k' given the history of measurements up to time step k, and is a combination of two independent point processes: a Poisson point process with density $f^p_{k'|k}(\cdot)$, and a multi-Bernoulli mixture (MBM) process with density $f^{mbm}_{k'|k}(\cdot)$, where $k' \in \{k, k+1\}$ correspond to the updated and predicted processes in the filter. The union of these two processes, i.e., a Poisson and an MBM processes, has been proven to be a conjugate prior with respect to the standard point target measurement model [3], [17].

The PMBM density is expressed over the union of the undetected targets set Y, and the detected target set W:

$$f_{k'|k}\left(X_{k'|k}\right) = \sum_{Y \uplus W = X} f^p_{k'|k}(Y) f^{mbm}_{k'|k}(W), \tag{1}$$

where the sum goes over all mutually disjoint sets Y and W, which have the property that their union is X.

The PPP density represents the undetected targets, i.e., targets that exist at the current time instant k', but have not yet been detected. This density is defined via

$$f^p_{k'|k}(X) = e^{-\int D_{k'|k}(x)\mathrm{d}x} \prod_{x \in X} D_{k'|k}(x), \tag{2}$$

where $D_{k'|k}(\cdot)$ is the intensity of a PPP. In a PPP, the number of targets is Poisson distributed and target states are independent, and identically distributed. The MBM component represents the potentially detected targets, and it can be described as [17]:

$$f^{mbm}_{k'|k}(X) = \sum_{a \in \mathcal{A}_{k'|k}} w^a_{k'|k} \sum_{\uplus_{j=1}^{n_{k'|k}} X^j = X} \prod_{i=1}^{n_{k'|k}} f^{i,a^i}_{k'|k}\left(X^i\right), \tag{3}$$

where i is the index over the Bernoulli components, $a = \left\{a^1, \ldots, a^{n_{k'|k}}\right\} \in \mathcal{A}_{k'|k}$ represents a specific data association hypothesis, $a^i \in \left\{1, \ldots, h^i_{k'|k}\right\}$ is an index over the $h^i_{k'|k}$ single target hypotheses for the i-th potential target/Bernoulli component, and $n_{k'|k}$ is the number of potentially detected targets. Each set of single target hypothesis $a \in \mathcal{A}_{k'|k}$ is also called a global hypothesis, and it is associated to a weight $w^a_{k'|k}$ satisfying $\sum_{a \in \mathcal{A}_{k'|k}} w^a_{k'|k} = 1$. The same single target hypotheses can appear in several global hypotheses.

The Bernoulli density corresponding to the i-th potential target and the a_i single target hypothesis $f^{i,a^i}_{k'|k}(X)$ can describe a newly detected target, or it can represent a previously detected target or false alarm; this makes it possible to efficiently model both the uncertainty regarding target existence and state. Mathematically, it can be expressed as

$$f^{i,a_i}_{k'|k}(X) = \begin{cases} 1 - r^{i,a^i}_{k'|k}, & X = \emptyset, \\ r^{i,a^i}_{k'|k} p^{i,a^i}_{k'|k}(x), & X = \{x\}, \\ 0, & \text{otherwise.} \end{cases}, \tag{4}$$

where $r^{i,a^i}_{k'|k} \in [0,1]$ is the probability of target existence and $p^{i,a^i}_{k'|k}(\cdot)$ is the state density provided that it exists.

In this work, we consider the Gaussian PMBM representation proposed in [3], where $p^{i,a^i}_{k'|k}(\cdot) = \mathcal{N}\left(\cdot; \bar{x}^{i,a^i}_{k'|k}, P^{i,a^i}_{k'|k}\right)$, with mean $\bar{x}^{i,a^i}_{k'|k}$ and variance $P^{i,a^i}_{k'|k}$. In this context, the MBM density is entirely defined by the following parameters

$$\left\{\left(w^a_{k'|k}, r^{i,a^i}_{k'|k}, \bar{x}^{i,a^i}_{k'|k}, P^{i,a^i}_{k'|k}\right)\right\}_{i \in \left\{1,\ldots,n_{k'|k}\right\}},$$

where $a \in \mathcal{A}_{k'|k}$ is defined in [17]. All details on the PMBM filtering recursion can be found in [3], [17]. The implementation we use in this paper requires the nonlinear filtering techniques in [13], also discussed in Section III-B.

III. Sonar surveillance model

From the perspective of the filtering algorithm, the detection process is modelled as a combination of true detection and false alarms. The probability of detection will be a function of the target state, which may include the target orientation for non-isotropic reflectors.

This section provides a probabilistic model of sonar surveillance process, including its detection part. We consider a sensor capable of providing noisy measurements of azimuth and range, and whose ability to detect targets is limited by the signal-to-noise (SNR) conditions in the area of surveillance and further complicated by the presence of false alarms. This model can be readily used to simulate sonar measurements for any given multi-target configuration, but it requires additional approximations [13] detailed further in order to fit into the Gaussian tracking algorithm of Section II.

A. Measurement model

The single-target state is represented as a vector $x = [p_x, v_x, p_y, v_y]^T$, where $[p_x, p_y]^T$ is the position vector and $[v_x, v_y]^T$ is the velocity vector. The sonar state is described by $s = \left[p^s_x, v^s_x, p^s_y, v^s_y\right]^T$.

1) Range-bearing measurements: The sonar in s measures azimuth, represented as a two-dimensional vector z_1 of length 1, and range z_2, such that $z = [z_1; z_2]$. The azimuth measurement z_1 is modelled as a von-Mises Fisher (VMF) distribution [18]

$$l(z_1|x) = \mathcal{V}(z_1; h(x), \kappa), \tag{5}$$

$$h(x) = \begin{bmatrix}\cos\varphi(x)\\ \sin\varphi(x)\end{bmatrix}, \tag{6}$$

$$\varphi(x) = \operatorname{atan2}(p_y - p_y^s, p_x - p_x^s), \tag{7}$$

where $\mathcal{V}(\cdot;\mu,\kappa)$ is the VMF density embedded in $\mathbb{R}^2$, w.r.t. the uniform distribution, with mean direction μ and concentration parameter $\kappa \geq 0$, and $\operatorname{atan2}(\cdot,\cdot)$ is the four-quadrant inverse tangent,. This density is

$$\mathcal{V}(z_1;\mu,\kappa) = \frac{\exp\left(\kappa\mu^T z_1\right)}{\mathrm{I}_0(\kappa)}\chi_{\|z_1\|=1}(z_1) \tag{8}$$

where $\mathrm{I}_a(\cdot)$ represents the modified Bessel function of the first kind and order $a, \Gamma(\cdot)$ represents the gamma function and $\chi_A(\cdot)$ is the indicator function on set A. The VMF distribution is unimodal for $\kappa > 0$ and uniform for $\kappa = 0$.

We consider Gaussian distribution for the range, so that the density of z_2 given x is

$$l(z_2|x) = \mathcal{N}\left(z_2; r(x), \sigma_r^2\right), \tag{9}$$

$$r(x) = \left\|\left[p_x - p_x^s, p_y - p_y^s\right]\right\|. \tag{10}$$

Given the state, the range and direction-of-arrival measurements are independent so

$$l(z|x) = l(z_1|x)\, l(z_2|x)$$

where $l(z_1|x)$ and $l(z_2|x)$ are given, respectively, by (5) and (9).

2) Detection uncertainty: Considering an amplitude receiver, the target signal is passed through a matched filter and an envelope detector, and target detection [19], i.e., a particular range-azimuth measurement, is declared if the received signal exceeds a certain threshold. Under assumption that the noise in the matched filter is narrowband Gaussian, the output to be thresholded is then Rayleigh distributed (Swerling I). The probability that target is detected in the received signal is then given by a well know expression

$$p_D(x) = p_{\mathrm{FA}}^{\frac{1}{1+\mathrm{SNR}(x;s)}}, \tag{11}$$

where p_{FA} is a desirable probability of a false alarm, and $\mathrm{SNR}(x;s)$ is the value of signal-to-noise ratio available to the receiver located in s when target is in x, and the probability of not detecting a target is then $1 - p_D(x)$.

3) False alarms: In addition to detection uncertainty, the sensor is prone to false range-bearing measurements, modelled by a PPP. The surveillance area covers the range interval $[r_{\min}, r_{\max}]$ and the interval of possible direction of arrivals $[\varphi_{\min}, \varphi_{\max}]$. The intensity function of false measurements $\lambda^{\mathrm{FA}}(\cdot)$ is uniform such that

$$\lambda^{\mathrm{FA}}\left(\left[z_1^T, z_2\right]^T\right) = \overline{\lambda}^{\mathrm{FA}} \cdot c\left(\left[z_1^T, z_2\right]^T\right), \tag{12}$$

where $\overline{\lambda}^{\mathrm{FA}}$ is the mean number of false measurements per scan, and $c(\cdot)$ is a density

$$c\left(\left[z_1^T, z_2\right]^T\right) = \mathcal{V}\left(z_1; [1,0]^T, 0\right)\mathcal{U}_{[r_{\min}, r_{\max}]}(z_2), \tag{13}$$

where $\mathcal{U}_{[r_{\min}, r_{\max}]}(\cdot)$ is a uniform density in the interval $[r_{\min}, r_{\max}]$. If a measurement z belongs to the surveillance area, we have $\lambda^{\mathrm{FA}}(z) = \overline{\lambda}^{\mathrm{FA}}(r_{\max} - r_{\min})^{-1}$.

B. Approximations in the filtering update step

Target tracking with the above model of surveillance implies tracking with non-linear non-Gaussian measurements and state-dependent probability of detection. This can be accomplished using either particle filtering techniques or Gaussian approximations. In this work we adopt a particular version of [3] that is based on Gaussian approximations reported in [13]. This approach uses the iterated posterior linearisation filter (IPLF) based on conditional moments to perform the single-target updates [20], [21], which requires the use of sigma-point integration methods [22]. A particular advantage of this algorithm in comparison to particle filtering is its lower computational complexity.

Specifically, these approximations are aimed at obtaining Gaussian densities describing the states of individual targets, and representing multi-target posteriors with sufficient precision. To approximate the single-target posterior and the normalising constant in the multi-target posterior, we need $l(z|x)$ and its conditional moments. The normalising constant with state-dependent probability of detection can be approximated by drawing sigma-points with respect to the posterior approximation. The exact details of this method can be found in [13].

IV. Simulation of active sonar with BELLHOP

This section develops an approach to describing the signal-to-noise conditions in the sonar surveillance area, as this is required for the state-dependent probability of target detection model in Section III-A2. The variations in SNR level will be primarily determined by the transmission loss accumulated by a sonar signal insonifying the surveillance area, as it is done to simulate sonar detections, e.g., in [7].

A. Simulating transmission loss in active sonar

This section describes the main characteristics of the BELLHOP software that models propagation of acoustic waves in underwater environment. For the purpose of this paper, we shall be interested in constructing the transmission loss values for an active sonar using the software's output.

1) The BELLHOP ray tracing model: The underwater environment is considered to be one of the most complex mediums for the transmission of signals. Due to this complexity, acoustic simulations are time consuming and computationally expensive, and it is desirable to have a model of signal propagation that is efficient and flexible at the same time. A useful description of how sound propagates through the underwater medium is provided by ray tracing models. To

determine the ray coordinates, i.e., to calculate the eigenrays, a solution of the ray equations is required.

BELLHOP is an industry standard ray tracing model for predicting acoustic pressure fields in ocean environments [10], [23]. BELLHOP offers the ability to simulate propagation of a sonar signal from its source to a receiver, which are both described by their locations in Cartesian coordinates, in a customisable underwater environment. BELLHOP is open source and written in FORTRAN, with a file based interface, where the scenario and the environmental conditions are contained in text files that BELLHOP uses as the source for the acoustic calculations. Typically, for sonar frequencies above $1\mathrm{kHz}$, the BELLHOP modelling is considered to be relatively representative of real sonar behaviour. It can be used to predict system performance and to generate complex waveforms [24]. BELLHOP can produce a variety of useful outputs, that are different (text) files depending on the options selected within the environmental file, and include transmission loss, eigenrays, arrival times, and receiver time series.

In this paper, we use the 3D version of BELLHOP (BELLHOP3D) to provide estimates for the attenuation of the sonar signals along the propagation paths, and to provide the resultant transmission loss for the active sonar signal propagating from the transmitter to the target and back from the target to the receiver array. For this project, an interface was developed to allow BELLHOP to be called by MATLAB, where the MATLAB automatically generated the BELLHOP data files for the scenario and the environment, and then extracted the relevant parameters from the BELLHOP output files.

TABLE I
PARAMETERS AND INFORMATION IN BELLHOP

Parameter
Source (S) position in 3D
Receiver (R) position in 3D
Declination angles (for R and S)
Azimuth angles (for R and S)
Number of top and bottom bounces
Amplitude
Transmission loss (in dB)
Delay (in sec)

2) Simulating transmission loss in active sonar: The BELLHOP model has been developed to describe acoustic ray propagation from a signal source to a hydrophone array that is spatially separated from the source. Such settings naturally represent the case of passive sonar, where the source represents a target; however, they require additional modification to model the operation of an active sonar. Specifically, modelling target insonification with a sonar signal can be done in two parts:

- simulating the transmission path from the source to the target and
- simulating the transmission path from the target to the receiver.

In the first part, a request to BELLHOP is sent where the position of the sonar platform is the source and the position of the target is the receiver. The direction of the beam and its width are defined by the properties of the actual sonar system considered. This BELLHOP request returns the propagation loss from source to target $\mathrm{TL}_{\text{S-T}}$, as well as other data as found in Table I. For the second request, the source and receiver are redefined such that the target's position is now the source and the sonar platform is the receiver (or, more generally, the receiver array, which could be an extended structure with hydrophones placed at multiple locations and is not necessarily co-located with the transmitter). In this case the target is assumed to be an omnidirectional source with a defined target strength to reflect the interaction of the incident acoustic waves with the target structure. Here the BELLHOP response provides us with the transmission loss from target to receiver that is $\mathrm{TL}_{\text{T-R}}$. Ultimately, the resulting transmission loss for a given pair of sonar and target states is the product of $\mathrm{TL}_{\text{S-T}}$ and $\mathrm{TL}_{\text{T-R}}$, or more typically, the sum of the transmission losses described in decibels.

B. Active sonar equation

The value of SNR available to the receiver is a function of a number of factors that are collected in form of a sonar equation, which is written (in dB) as

$$\mathrm{SNR}(x;s) = \textsc{signal}(x;s) - \textsc{noise}, \tag{14}$$

where SIGNAL and NOISE represent the power of the received signal and noise, respectively. For an active sonar, these components are

$$\textsc{signal}(x;s) = \mathrm{SL} - (\mathrm{TL}(x;s) - \mathrm{TS}), \tag{15}$$

$$\textsc{noise} = \mathrm{NL} - \mathrm{AG}, \tag{16}$$

and where SL is the Source Level for the transducer, TS is the target strength, NL is the ambient noise level, AG is the array gain (related to the directionality of the array), and $\mathrm{TL}(x;s) = \mathrm{TL}_{\text{S-T}}(x;s) + \mathrm{TL}_{\text{T-R}}(x;s)$ can be evaluated through BELLHOP ray tracing model for particular propagation conditions as specified by the environmental file, and with specific values measured in decibels relative to the standard reference intensity of a $1\mu\mathrm{Pa}$ plane waves. Overall, equation (14) can be read as the sound history of an active sonar: a wave is first transmitted by the transducer with a certain energy SL, the emitted wave propagates into the medium, its energy decreases along the propagation $\mathrm{TL}_{\text{S-T}}$. The sound wave interacts with a target and a part of the energy is reflected back toward the sonar TS. And finally the target echo propagates back to the receiver losing energy along the path $\mathrm{TL}_{\text{T-R}}$.

V. EXPERIMENTAL RESULTS

We proceed to assess the developed sonar tracking algorithm. The approach taken in this paper is to contrast performance attained using the true probability model against that obtained with uniform probability of detection, which recreates the situation when true model is not available to the filter.

TABLE II
INITIAL TARGET STATES AND TRACK INFORMATION.

Init.loc. (m)	Init.vel. (ms^{-1})	Time of birth/death (s)
$[-126.30, 1585.60]^T$	$[0.86, 3.76]^T$	6/40
$[890.86, 1797.07]^T$	$[-0.13, 0.47]^T$	15/40
$[-72.74, 1984.99]^T$	$[-1.88, -3.79]^T$	24/40
$[222.30, 1386.92]^T$	$[-2.24, -2.20]^T$	33/40

A. Simulation details

Experimental results produced in this work are based on the following models of target dynamics and sonar measurements. A set of parameters used to configure the PMBM filtering algorithm is also provided.

a) Multi-target dynamics: Targets move with probability of survival $p_S = 0.99$ and a nearly constant velocity model with transition density

$$g(\cdot|x) = \mathcal{N}(\cdot; Fx, Q), \tag{17}$$

$$F = I_2 \otimes \begin{pmatrix} 1 & \tau \\ 0 & 1 \end{pmatrix}, \; Q = qI_2 \otimes \begin{pmatrix} \tau^3/3 & \tau^2/2 \\ \tau^2/2 & \tau \end{pmatrix} \tag{18}$$

where $\otimes$ is the Kronecker product, $\tau = 10\mathrm{s}$ is the sampling period and $q = 0.001\mathrm{m}^2\mathrm{s}^{-3}$ is the variance of velocity increments.

The intensity of the PPP birth process is Gaussian with mean $\bar{x}_k^b = [0, 0, 2000, 0]^T$ and covariance matrix $P_k^b = \mathrm{diag}([400^2, 2^2, 400^2, 2^2])$, and rate $w^b = 0.05$.

b) Sonar measurements: A stationary sonar is located at the origin, and the surveillance area is limited to $[r_{\min}, r_{max}] = [1000\mathrm{m}, 3000\mathrm{m}]$, and $[\varphi_{\min}, \varphi_{\max}] = [\frac{\pi}{3}, \frac{2\pi}{3}]$. The VMF distributed azimuth noise is characterised by a concentration parameter κ, that is selected to correspond to a Gaussian distribution with standard deviation $\sigma_\varphi = \frac{\pi}{180}$ via $\kappa = \sigma_\varphi^{-2}$. The range noise is zero-mean Gaussian with standard deviation $\sigma_r = 20\mathrm{m}$.

The sonar's probability of detection for a target in a given state is evaluated using (11) with the SNR computed as (14), where transmission losses are evaluated based on the BELLHOP simulation. Simulating the sonar operating at $1\mathrm{kHz}$ at depth $80\mathrm{m}$ and the depth of bottom $150\mathrm{m}$, the resulting probability of detection is as in Figure 1. The probability of detection outside the surveillance area is set to 0 in the computations, as in [6]. The false alarm model is Poisson, uniformly distributed in the surveillance area, with a mean number of false measurements per scan equal to $\lambda = 10$.

c) Filtering implementation: We consider the PMBM filtering algorithm in Section II with Gaussian approximations in Section III. In the considered implementation the maximum number of global hypotheses is set to $N_h = 500$, threshold for pruning the Poisson components $\Gamma_p = 10^{-5}$, threshold for pruning global hypotheses $\Gamma_{mbm} = 10^{-6}$, and threshold for pruning Bernoulli components $\Gamma_b = 10^{-6}$. The ellipsoidal gating is performed with a threshold equal to 200, while the state extraction is performed by selecting the global hypothesis that has the highest weight and then reporting the means of Bernoulli components whose existence probability is above 0.4 [3, Sec. VI.A]. Finally, in these experiments we use the measurement driven initial linearization and the number of iterations of the IPLF is set to 1.

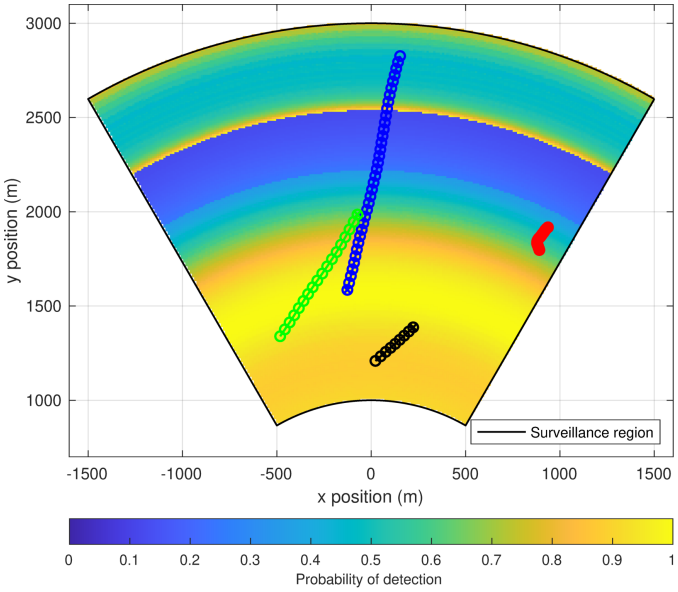

Fig. 1. Probability of target detection with an active sonar as evaluated using the BELLHOP simulation over a limited surveillance region. The sonar location is at the origin (not depicted). It may appear counter-intuitive that probability of detection does not strictly decrease with distance, as e.g., in [6], for the considered depth, but this pattern emerges due to non-straight line propagation of sonar signals, which may travel across various depths while accumulating propagation loss before arriving at the considered depth. This figure also features true target trajectories that are used in the experiments.

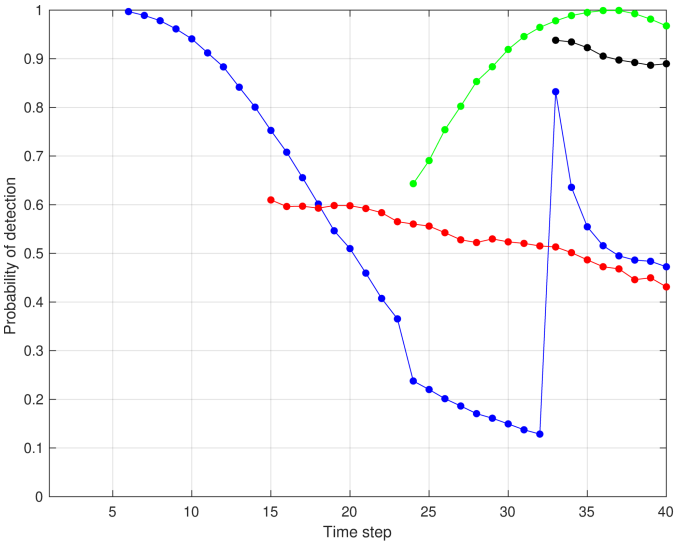

Fig. 2. The actual values of probability of detection along the targets' trajectories that are used for generating the sonar measurements (or detection failures) in the experiments.

This implementation, when compared to [13], employs a higher number of global hypotheses and lower pruning thresholds, which preserves richer information on the multi-target configuration within the filter. Specifically, this makes it possible for the filter to track a target through the areas of low probability of detection, where target is only detected sporadically—possibly, with several time steps separating suc-

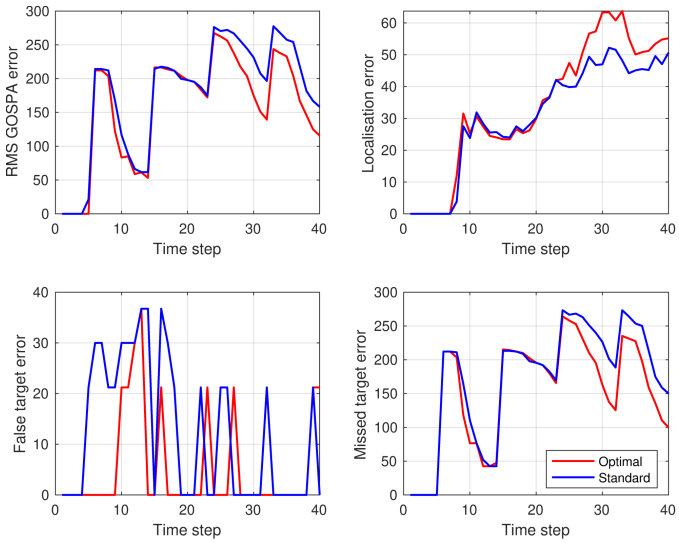

Fig. 3. RMS GOSPA error against time and its decompositions for the standard and optimal implementation of the PMBM filter. Results are generated for false alarm rate $\lambda^{\text{FA}} = 10$ and averaged over 100 Monte Carlo runs.

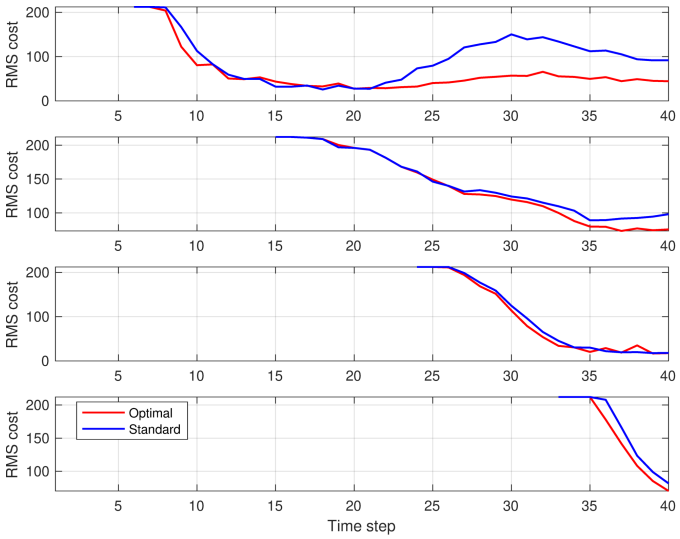

Fig. 4. RMS localisation and missed target cost against time for each of the 4 ground truth trajectories. Results are generated for false alarm rate $\lambda^{\text{FA}} = 10$ and averaged over 100 Monte Carlo runs.

cessive detections,—and otherwise may be at risk of having its associated Bernoulli components pruned prematurely.

B. Performance comparison

We assess performance of a PMBM filter that is informed about the sonar's probability of detection model $p_D(\cdot)$, referred to as the *optimal* algorithm next, and compare it to the *standard* algorithm, which (incorrectly) assumes the probability of detection to be uniform over surveillance area. In both standard and optimal algorithm just a low number of points are queried in the update step to access the probability of detection. In this implementation of the PMBM filter the probability of detection is evaluated in 7 characteristic points for each Bernoulli-Gaussian in the predicted MBM describing the surviving targets, as well as for a single Gaussian that characterises the spatial distribution of a Poisson process describing the undetected targets [21].

In the standard algorithm, the value of probability of detection is set to $p_D = 0.66$, and is obtained from the BELLHOP model as the average probability value across all ranges within $[r_{\min}, r_{\max}]$. For the optimal algorithm, we precompute the probability of detection in a grid of ranges, i.e., employ a lookup table, to further alleviate the computational burden associated with that BELLHOP is not an optimised ray tracing code. Then, the tracker accesses probability in a nearest point on the grid in place of evaluating each point in BELLHOP — the grid spacing is sufficiently fine that interpolation is not necessary in the cases considered.

The considered scenario lasts for 40 time steps, and consists of total 4 targets that are generated from the birth model described in Section V-A. The resulting initial target states are given in Table II, and targets follow trajectories as depicted on Figure 1. In this scenario, the probability of detecting a target varies along its respective trajectory (see Figure 2), and typically deviates from the value $p_D = 0.66$ that is assumed by the standard algorithm.

These two PMBM algorithms, i.e., the optimal and standard ones, have been applied to sonar data generated using the sonar model in Section V-A. In order to evaluate their tracking performance, the Generalized Optimal Sub-Pattern Assignment (GOSPA) metric [25] per time step is used with the Euclidean distance (i.e. $p = 2$) and the cutoff $c = 300\text{m}$, the parameter is set to $\alpha = 2$, which allows to decompose the total error into three components: localization error, missed target error and false target error. The RMS GOSPA metric errors against time are shown in Figure 3.

The best performing algorithm is the optimal algorithm, its RMS GOSPA error is predominantly the same or lower than that of the standard algorithm. This confirms an intuition that communicating the true probability of detection model to the filter is an important factor to improve tracking performance. A closer inspection of the GOSPA components reveals that optimal algorithm is superior in situations when there are targets operating in the areas of low probability of detection, and there is a possibility of missing a target because of that. This is specifically pronounced in terms of missed target error, starting from time step 24. However, the resulting estimates (when reported) may not be very accurate, as seen through localisation error. Finally, both algorithms behave in the same manner with respect to false alarms. The false alarm contribution to the total error is considerably lower than the missed target error, indicating that filters tend to miss more targets than to report false targets.

In order to comment on what types of trajectories are most likely to benefit from the use of the BELLHOP model, for each target we consider the values of a cost function (see Figure 4), which can quantify both failures to report a target's existence as well as localisation errors for a reported target. The resulting cost values confirm that performance improvement is gained by the optimal algorithm in the areas with low probability of detection; notably, after time step 21 for target 1 and after time step 30 for target 2. It also reveals that for target 4 that operates

in the area of high probability of detection, not having access to the BELLHOP model leads to performance degradation due to delayed track confirmation in presence of false alarms.

This cost function that is considered above for individual targets is computed similarly to the GOSPA metric [25], and uses the same set of configuration parameters. Specifically, at each time step, an optimal assignment is established between the set of ground truth target states and the set of target estimates. For each true target, if the assigned estimate is within the cut-off distance c, the cost function simply evaluates to Euclidean distance. Otherwise, if no estimate is associated to this target (or if the distance between the true target and its estimate is bigger than c), the cost function evaluates to $c/\alpha^{1/p}$.

VI. Conclusion

In this paper we have presented an efficient approach to multi-target filtering with an active sonar. Its novelty in that it takes into account sonar's state-dependent probability of target detection, which is generally not uniform across the surveillance area and cannot be expressed through a simple analytical expression. The approach is enabled by a particular implementation of the PMBM filter, which requires only a limited number of location points to evaluate the probability of detection, and the model of probability of detection that is based on sonar simulations performed with the BELLHOP model.

Previous work has commonly assumed that the probability of detection model is uniform across the surveillance area. As expected, using a realistic sonar model within the filter improves tracking performance.

Further work to extend this work will include taking the peculiarities of the underwater environment into account to calculate range measurements using the BELLHOP simulation and an analysis of the types of environment and trajectories for which the use of realistic sonar models is important for tracking performance.

Acknowledgement

The authors would like to thank DSTL Grant no. 1000143726 for financial support.

References

[1] D. Reid, "An algorithm for tracking multiple targets," *IEEE transactions on Automatic Control*, vol. 24, no. 6, pp. 843–854, 1979.

[2] J. L. Williams, "Hybrid poisson and multi-Bernoulli filters," in *2012 15th International Conference on Information Fusion*, pp. 1103–1110, IEEE, 2012.

[3] Á. F. García-Fernández, J. L. Williams, K. Granström, and L. Svensson, "Poisson multi-Bernoulli mixture filter: direct derivation and implementation," *IEEE Transactions on Aerospace and Electronic Systems*, vol. 54, no. 4, pp. 1883–1901, 2018.

[4] E. Brekke and M. Chitre, "Relationship between finite set statistics and the multiple hypothesis tracker," *IEEE Transactions on Aerospace and Electronic Systems*, vol. 54, no. 4, pp. 1902–1917, 2018.

[5] M. A. Ainslie, *Principles of sonar performance modelling*, vol. 707. Springer, 2010.

[6] G. Hendeby and R. Karlsson, "Gaussian mixture PHD filtering with variable probability of detection," in *17th International Conference on Information Fusion (FUSION)*, pp. 1–7, IEEE, 2014.

[7] R. Georgescu and P. Willett, "The GM-CPHD tracker applied to real and realistic multistatic sonar data sets," *IEEE Journal of Oceanic Engineering*, vol. 37, no. 2, pp. 220–235, 2012.

[8] F. Ehlers, M. Daun, and M. Ulmke, "System design and fusion techniques for multistatic active sonar," in *OCEANS 2009-EUROPE*, pp. 1–10, IEEE, 2009.

[9] B. Liu, X. Tang, R. Tharmarasa, T. Kirubarajan, R. Jassemi, and S. Hallé, "Underwater target tracking in uncertain multipath ocean environments," *IEEE Transactions on Aerospace and Electronic Systems*, vol. 56, no. 6, pp. 4899–4915, 2020.

[10] M. B. Porter, "The BELLHOP manual and user's guide: Preliminary draft," *Heat, Light, and Sound Research, Inc., La Jolla, CA, USA, Tech. Rep*, vol. 260, 2011.

[11] W. R. Blanding, P. K. Willett, Y. Bar-Shalom, and R. S. Lynch, "Directed subspace search ML-PDA with application to active sonar tracking," *IEEE Transactions on Aerospace and Electronic Systems*, vol. 44, no. 1, pp. 201–216, 2008.

[12] D. Musicki, X. Wang, R. Ellem, and F. Fletcher, "Efficient active sonar multitarget tracking," in *OCEANS 2006-Asia Pacific*, pp. 1–8, IEEE, 2006.

[13] A. F. Garcia-Fernandez, J. Ralph, P. Horridge, and S. Maskell, "A Gaussian filtering method for multi-target tracking with nonlinear/non-Gaussian measurements," *IEEE Transactions on Aerospace and Electronic Systems*, pp. 1–1, 2021.

[14] X. Wang, D. Musicki, R. Ellem, and F. Fletcher, "Efficient and enhanced multi-target tracking with doppler measurements," *IEEE Transactions on Aerospace and Electronic Systems*, vol. 45, no. 4, pp. 1400–1417, 2009.

[15] Y. Pailhas, J. Houssineau, Y. R. Petillot, and D. E. Clark, "Tracking with MIMO sonar systems: applications to harbour surveillance," *IET Radar, Sonar & Navigation*, vol. 11, no. 4, pp. 629–639, 2017.

[16] R. P. Mahler, *Advances in statistical multisource-multitarget information fusion*. Artech House, 2014.

[17] J. L. Williams, "Marginal multi-Bernoulli filters: RFS derivation of MHT, JIPDA, and association-based MeMBer," *IEEE Transactions on Aerospace and Electronic Systems*, vol. 51, no. 3, pp. 1664–1687, 2015.

[18] K. V. Mardia, P. E. Jupp, and K. Mardia, *Directional statistics*, vol. 2. Wiley Online Library, 2000.

[19] T. Kirubarajan and Y. Bar-Shalom, "Low observable target motion analysis using amplitude information," *IEEE Transactions on Aerospace and Electronic Systems*, vol. 32, no. 4, pp. 1367–1384, 1996.

[20] F. Tronarp, A. F. Garcia-Fernandez, and S. Särkkä, "Iterative filtering and smoothing in nonlinear and non-Gaussian systems using conditional moments," *IEEE Signal Processing Letters*, vol. 25, no. 3, pp. 408–412, 2018.

[21] Á. F. García-Fernández, F. Tronarp, and S. Särkkä, "Gaussian target tracking with direction-of-arrival von mises–fisher measurements," *IEEE Transactions on Signal Processing*, vol. 67, no. 11, pp. 2960–2972, 2019.

[22] S. Särkkä, *Bayesian filtering and smoothing*. Cambridge university press, 2013.

[23] O. C. Rodriguez, "General description of the BELLHOP ray tracing program," *Physics Department Signal Processing Laboratory Faculty of Sciences and the University of the Algarve Tecnologia (Galician), Version*, vol. 1, 2008.

[24] A. I. Larsson and C. Gillard, "On waveform selection in a time varying sonar environment," *Proc. of Acoust*, pp. 72–78, 2004.

[25] A. S. Rahmathullah, Á. F. García-Fernández, and L. Svensson, "Generalized optimal sub-pattern assignment metric," in *2017 20th International Conference on Information Fusion (Fusion)*, pp. 1–8, IEEE, 2017.